

Interference between $f_0(980)$ and $\rho(770)^0$ resonances in $B \rightarrow \pi^+\pi^-K$ decays

B. El-Bennich,¹ A. Furman,² R. Kamiński,³ L. Leśniak,³ and B. Loiseau¹

¹*Laboratoire de Physique Nucléaire et de Hautes Énergies (IN2P3-CNRS-Universités Paris 6 et 7),
Groupe Théorie, Université Pierre et Marie Curie, 4 place Jussieu, 75252 Paris, France*

²*ul. Bronowicka 85/26, 30-091 Kraków, Poland*

³*Division of Theoretical Physics, The Henryk Niewodniczański Institute of Nuclear Physics,
Polish Academy of Sciences, 31-342 Kraków, Poland*

(Dated: December 24, 2018)

We study the contribution of the strong interaction between the two pions in S - and P -waves to the weak $B \rightarrow \pi\pi K$ decay amplitudes. The interference between these two waves is analyzed in the $\pi\pi$ effective mass range of the $\rho(770)^0$ and $f_0(980)$ resonances. We use a unitary $\pi\pi$ and $\bar{K}K$ coupled-channel model to describe the S -wave interactions and a Breit-Wigner function for the P -wave amplitude. The weak B -decay amplitudes, obtained from QCD factorization, are supplemented with charming penguin contributions in both waves. The four complex parameters of these long distance terms are determined by fitting the model to the BaBar and Belle data on $B^{\pm,0} \rightarrow \pi^+\pi^-K^{\pm,0}$ branching fractions, CP asymmetries, $\pi\pi$ effective mass and helicity-angle distributions. This set of data, and in particular the large direct CP -asymmetry for $B^\pm \rightarrow \rho(770)^0 K^\pm$ decays, is well reproduced. The interplay of charming penguin amplitudes and the interference of S - and P -waves describes rather successfully the experimental \mathcal{S} and \mathcal{A} values of the CP -violating asymmetry for both $B^0 \rightarrow f_0(980)K_S^0$ and $B^0 \rightarrow \rho(770)^0 K_S^0$ decays.

PACS numbers: 13.25.Hw, 13.75Lb

I. INTRODUCTION

Hadronic final-state interactions in three-body charmless B meson decays supply good opportunities for CP violation searches. In order to interpret in the most reliable way decay observables, it is necessary to take into account strong interaction effects between the produced meson pairs. These effects, at relative energies below and about 1 GeV, are clearly visible in the Dalitz plots of three-body weak decays such as $B \rightarrow \pi\pi K$ and $B \rightarrow \bar{K}KK$ [1–6]. In particular, one observes a distinct surplus of events at these relatively small effective masses distributed near the edge of the Dalitz plot. Prominent maxima are seen in the effective $\pi\pi$ mass distribution, notably the $f_0(980)$ and $\rho(770)^0$ resonances. Several resonances at higher energies are visible too, though their identification is less straightforward. In phenomenological studies of B meson decays, the isobar model is employed, which has a large number of arbitrary phases and relative intensity parameters. One of our aims is to reduce this number of free parameters by using a model which describes many resonances in a unitarized way.

In Ref. [7], particular attention was paid to the $B \rightarrow f_0(980)K$ channels which have relatively large branching ratios for charmless B decays. Contributions from QCD factorization amplitudes solely do not reproduce the $B^\pm \rightarrow f_0(980)K^\pm$ and $B^0 \rightarrow f_0(980)K^0$ branching ratios. Therefore, additional terms were included in the decay amplitudes in the form of long-distance contributions stemming from so-called charming penguins [8]. At the hadronic level, these contributions could be associated with intermediate $D_s^{(*)}D^{(*)}$ states and be understood as being part of the intricate final-state interactions in B decays. The addition of charming penguins in

Ref. [7] allows to obtain a good agreement with the measured $B \rightarrow f_0(980)K$ branching ratios and to reproduce the effective $\pi\pi$ mass distribution of the BaBar and Belle data.

Long distance contributions, similar to the charming penguin effects, have been considered by Cheng, Chua and Soni [9]. Cheng, Chua and Yang have recently studied the nature of the scalar mesons $f_0(980)$ and $a_0(980)$ in the decays $B \rightarrow f_0(980)K$, $B \rightarrow a_0(980)\pi$ and $B \rightarrow a_0(980)K$ using QCD factorization for the weak decay amplitudes [10]. Their calculations are for a $\bar{q}q$ state of the $f_0(980)$, but implications of a $q^2\bar{q}^2$ picture of the $f_0(980)$ are also discussed. In their work [10], however, they neither consider hadronic long-distance contributions nor pionic and kaonic final-state interactions.

In the literature, one finds different results on the relative size of the weak annihilation or hard-spectator contributions to the B -decay amplitude into two mesons [11–13]. A recent study in soft-collinear effective theory [11] concludes that the annihilation and chirally enhanced annihilation contributions in charmless $B \rightarrow M_1 M_2$ decays are real to leading order in Λ_{QCD}/m_b (here M_1 and M_2 are non-isosinglet mesons, Λ_{QCD} is the QCD scale and m_b the b -quark mass). These contributions constitute a small fraction of the experimentally determined total penguin amplitudes in the case $\bar{B}^0 \rightarrow K^-\pi^+$ or $B^- \rightarrow K^-\bar{K}^0$ decays and in the present work they are not considered. Even upon inclusion of the relatively small annihilation and hard-spectator contributions, the current QCD factorization results underestimate the average branching ratio for $B \rightarrow \rho K$ by a factor of two and larger [14, 15] unless certain model parameters are strongly modified (see scenarios S2 to S4 in Ref. [15]). To be more quantitative, let us cite the branching ratio

of the $B^- \rightarrow K^- \rho^0$ decay calculated by Leitner, Guo and Thomas [14]. Including fully the two contributions, it is equal to 1.54×10^{-6} . This should be compared to the experimental branching ratio for this decay which lies between 3.9×10^{-6} and 5.1×10^{-6} with a typical error of 0.5×10^{-6} [1, 4].

In this paper, we supplement the $B \rightarrow \rho(770)^0 K$, $\rho(770)^0 \rightarrow \pi^+ \pi^-$ decay amplitudes to the $B \rightarrow f_0(980)K$, $f_0(980) \rightarrow \pi^+ \pi^-$ amplitudes derived in Ref. [7]. The experimental branching ratio for the decay $B \rightarrow \rho(770)^0 K$ is of the same order of magnitude as for the $B \rightarrow f_0(980)K$ channel. A characteristic feature of the $B^\pm \rightarrow \rho(770)^0 K^\pm$ decay, however, is the very large value of the direct CP violating asymmetry of about 0.3 measured by Belle [1] and BaBar [4]. The addition of the $B \rightarrow \rho(770)^0 K$ decay amplitudes enables us to study possible interferences between the S - and P -waves in $B \rightarrow \pi\pi K$ decays. These effects can be observed in particular in the time dependent CP asymmetries of neutral B decays into $\rho(770)^0 K_S^0$ and $f_0(980)K_S^0$ channels. In $b \rightarrow s$ transitions, *new physics* contributions to these asymmetries have been put forward [16, 17]. Nonetheless, one should also take into account the influence of meson-meson final-state interactions on these observables, among others on the deviation of the asymmetry parameter \mathcal{S} from the Standard Model expectation value $\sin 2\beta$.

In Section II, after a concise summary of the S -wave contributions $B \rightarrow f_0(980)K$ of Ref. [7], we derive the $B \rightarrow \rho(770)^0 K$ decay amplitudes from the QCD factorization approach of Ref. [15]. We introduce a Breit-Wigner vertex function $\Gamma_{\rho\pi\pi}(m_{\pi\pi}^2)$ in the $B \rightarrow \rho(770)^0 K$ decay amplitude to account for the $\pi\pi$ final-state interactions in the P -wave. We complement this amplitude with the S -wave contribution $B \rightarrow f_0(980)K$ obtained in Ref. [7]. In Section III, we give our model expressions for the observables measured by the Belle and BaBar Collaborations. We briefly discuss our fitting method in Section IV. In Section V our results are compared to the experimental $\pi\pi$ mass and helicity-angle distributions and we give our branching ratio values for $B \rightarrow \rho(770)^0 K$ and $B \rightarrow f_0(980)^0 K$ decays. We analyze the S - and P -wave interference effects as well as the influence of charming penguins on the CP violating parameters $\mathcal{S}(m_{\pi\pi})$ and $\mathcal{A}(m_{\pi\pi})$ of the time-dependent asymmetry in neutral B^0 decays. Furthermore, we calculate the asymmetry parameters \mathcal{S} and \mathcal{A} and compare our results with experimental data. Finally, in Section VI, we summarize and propose further improvements of this work.

II. AMPLITUDES FOR THE $B \rightarrow \pi\pi K$ DECAYS

A. A brief recall of the $B \rightarrow f_0(980)K$ amplitudes

In Ref. [7], the B decays into $\pi\pi K$ and $\bar{K}KK$ were studied for final-state $(\pi\pi)_S$ and $(\bar{K}K)_S$ pairs interact-

ing in an isospin zero S -wave from $\pi\pi$ threshold to about 1.2 GeV. The QCD factorization approach is the framework used to describe weak decays of B mesons into a quasi two-body state $f_0(980)K$. The effective coefficients $a_i(\mu)$ ($i = 1, \dots, 6$) at the renormalization scale $\mu = 2.1$ GeV were taken from Ref. [18]. Small corrections arising from annihilation topologies and hard gluon scattering with the spectator quark were not included.

The two-pion and two-kaon rescattering effects are described by the $\pi\pi$ and $\bar{K}K$ unitary coupled-channel model of Ref. [19], which allows to describe the lowest scalar-isoscalar resonances $f_0(600)$ and $f_0(980)$ with a single matrix of amplitudes. The meson-meson amplitudes are incorporated into four scalar form factors responsible for the production of the $\pi\pi$ and $\bar{K}K$ pairs in an isospin zero S -wave from the current $\bar{u}u, \bar{d}d$ and $\bar{s}s$ antiquark-quark states. These scalar form factors are constrained by the chiral dynamics of low-energy meson-meson interactions [20] and provide the link between the weak decay amplitudes [18] and the hadronic rescattering model [19].

As mentioned in the introduction, charming penguin amplitudes were included. In a nutshell, these amplitudes are low-momentum $\bar{c}c$ loop contributions which are formally suppressed by powers of Λ_{QCD}/m_b though numerically enhanced by large Wilson coefficients [8]. No explicit calculations being available so far, one interprets these amplitudes as long distance contributions parameterized by two complex parameters.

B. The $B \rightarrow \rho K, \rho \rightarrow (\pi\pi)_P$ decay amplitudes

The derivation of the $B \rightarrow \rho(770)^0 K$ weak decay amplitude follows the QCD factorization approach of Beneke and Neubert [15]. By $(\pi\pi)_P$ we denote isovector $\pi\pi$ states in a P -wave and in the following we will write interchangeably $\rho(770)^0$ or $(\pi\pi)_P$ depending on the context. The possible quark line diagrams for negative B -meson decays are shown in Fig. 1, where the $\pi^+ \pi^-$ final state interaction is graphically schematized by dashed lines appended to either a $\bar{u}u$ or $\bar{d}d$ state in the diagrams.

The $B^- \rightarrow (\pi^+ \pi^-)_P K^-$ decay amplitude can be written as

$$\langle (\pi^+ \pi^-)_P K^- | H | B^- \rangle = p_K \cdot (p_{\pi^-} - p_{\pi^+}) A^- \Gamma_{\rho\pi\pi}(m_{\pi\pi}), \quad (1)$$

where p_K is four-momentum of K^- and p_{π^-} and p_{π^+} are the four-momenta of the negative and positive pions, respectively. In the $\pi^+ \pi^-$ rest frame, the decay amplitude reduces to

$$\begin{aligned} \langle (\pi^+ \pi^-)_P K^- | H | B^- \rangle &= 2 A^- \Gamma_{\rho\pi\pi}(m_{\pi\pi}) |\mathbf{p}_\pi| |\mathbf{p}_K| \cos \theta, \end{aligned} \quad (2)$$

where $|\mathbf{p}_\pi|$ and $|\mathbf{p}_K| = \sqrt{E_K^2(m_{\pi\pi}) - m_K^2}$ are the moduli of the pion and kaon momenta with $E_K(m_{\pi\pi}) = \frac{1}{2}(M_B^2 - m_{\pi\pi}^2 - m_K^2)/m_{\pi\pi}$, M_B , $m_{\pi\pi}$ and m_K being the B -

meson, effective $\pi\pi$ and kaon masses, respectively. Moreover, θ is the helicity angle between the direction of flight of the π^- in the $\pi^+\pi^-$ rest frame and the direction of the $\pi^+\pi^-$ system in the B rest frame.

The function A^- is given by

$$A^- = G_F m_\rho [f_K A_0^{B \rightarrow \rho}(m_K^2) (U^- - C^P) + f_\rho F_1^{B \rightarrow K}(m_\rho^2) W^-], \quad (3)$$

where G_F is the Fermi coupling constant, $f_K = 159.8$ MeV is the kaon decay constant and the ρ decay constant is given by $f_\rho = 209$ MeV. For the transition form factors $B \rightarrow \rho$ and $B \rightarrow K$, we employ $A_0^{B \rightarrow \rho}(m_K^2) = 0.37$ and $F_1^{B \rightarrow K}(m_{\pi\pi}^2) = 0.34$, respectively. The above values for decay constants and transition form factors are taken from Table I of Ref. [15]. The functions U^- and W^- are defined as

$$U^- = \lambda_u [a_1 + a_4^u - a_4^c - r(a_6^u - a_6^c + a_8^u - a_8^c) + a_{10}^u - a_{10}^c] + \lambda_t [-a_4^c + r(a_6^c + a_8^c) - a_{10}^c] \quad (4)$$

and

$$W^- = \lambda_u a_2 - \lambda_t \times \frac{3}{2}(a_7 + a_9). \quad (5)$$

The chiral factor is given by $r = 2M_K^2/[(m_b + m_u)(m_s + m_u)]$, with $m_b = 4.46$ GeV and where $m_u = 5$ MeV and $m_s = 110$ MeV are the u - and s -quark masses, respectively. The coefficients $a_i(\mu = \frac{m_b}{2})$ are taken from Table III in Ref. [21]. In Eq. (4), we did not include the annihilation contribution considered in Ref. [15]. The charming penguin contribution C^P in Eq. (3) is parameterized as

$$C^P = \lambda_u P_u + \lambda_t P_t, \quad (6)$$

with P_u and P_t being complex parameters [8]. In Eqs. (4), (5) and (6), we have used the unitarity condition $\lambda_c + \lambda_u + \lambda_t = 0$, where $\lambda_u = V_{ub}V_{us}^*$, $\lambda_t = V_{tb}V_{ts}^*$ and $\lambda_c = V_{cb}V_{cs}^*$ are products of the Cabibbo–Kobayashi–Maskawa (CKM) matrix elements, to express the amplitudes in terms of λ_u and λ_t . The parameters of the CKM matrix are taken from Ref. [22].

The corresponding A^+ function of the $B^+ \rightarrow (\pi^-\pi^+)P K^+$ decay amplitude is obtained from replacing the λ_u and λ_t values by their complex conjugates λ_u^* and λ_t^* in Eqs. (4) to (6) and changing the overall sign in Eq. (2),

$$\langle (\pi^-\pi^+)P K^+ | H | B^+ \rangle = 2A^+ \Gamma_{\rho\pi\pi}(m_{\pi\pi}) |\mathbf{p}_\pi| |\mathbf{p}_K| \cos \theta, \quad (7)$$

where we define

$$A^+ = -A^-(\lambda_u^*, \lambda_t^*). \quad (8)$$

The minus sign in Eq. (8) follows from the CP symmetry of the final state.

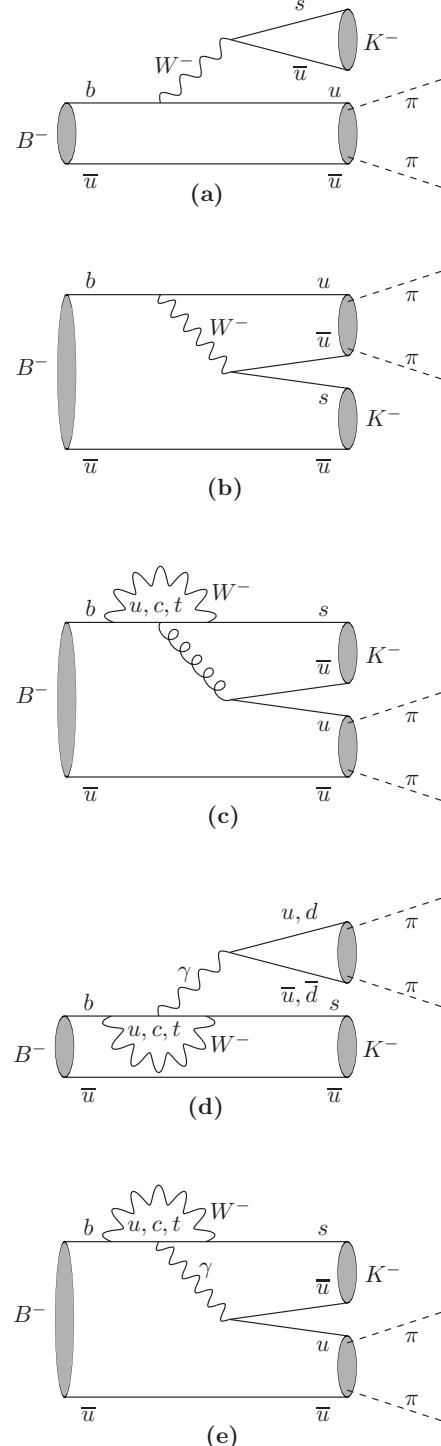


FIG. 1: Quark line diagrams for the B^- decay: (a) and (b) are tree diagrams, (c) is the penguin diagram and (d) and (e) are electroweak penguin diagrams. The spring-like lines represent gluon exchange, wavy lines photon or W^- exchange and the dashed ones the $\pi\pi$ isospin 1 P -wave pair.

Coming to neutral B decays, the $\bar{B}^0 \rightarrow \rho(770)^0 \bar{K}^0$,

$\rho^0 \rightarrow (\pi^+ \pi^-)_P$ decay amplitude reads

$$\begin{aligned} \langle (\pi^+ \pi^-)_P \bar{K}^0 | H | \bar{B}^0 \rangle \\ = 2 \bar{A}^0 \Gamma_{\rho \pi \pi}(m_{\pi \pi}) |\mathbf{p}_\pi| |\mathbf{p}_K| \cos \theta, \end{aligned} \quad (9)$$

with

$$\begin{aligned} \bar{A}^0 = G_F m_\rho \left[f_K A_0^{B \rightarrow \rho}(m_K^2) (\bar{U}^0 + C^P) \right. \\ \left. + f_\rho F_1^{B \rightarrow K}(m_\rho^2) \bar{W}^0 \right]. \end{aligned} \quad (10)$$

The different sign in front of the charming penguin term C^P is due to the $\bar{d}d$ quark content of the $\rho(770)^0$ in neutral B decays in contrast to Eq. (3), where in charged B decays the $\bar{u}u$ configuration comes into play. The function \bar{U}^0 is given by

$$\begin{aligned} \bar{U}^0 = \lambda_u \{ -a_4^u + a_4^c + r [a_6^u - a_6^c - (a_8^u - a_8^c)/2] \\ + (a_{10}^u - a_{10}^c)/2 \} + \lambda_t [a_4^c - r(a_6^c - a_8^c/2) - a_{10}^c/2] \end{aligned} \quad (11)$$

and $\bar{W}^0 = W^-$. Here again we have left out annihilation contributions as considered in Ref. [15]. The replacement of λ_u and λ_t by their complex conjugate values in Eqs. (5) and (11) leads to the corresponding function A^0 for the $B^0 \rightarrow (\pi^- \pi^+)_P K^0$ decays which reads

$$\begin{aligned} \langle (\pi^- \pi^+)_P K^0 | H | B^0 \rangle \\ = 2 A^0 \Gamma_{\rho \pi \pi}(m_{\pi \pi}) |\mathbf{p}_\pi| |\mathbf{p}_K| \cos \theta, \end{aligned} \quad (12)$$

where one has again to account for an overall sign change in the amplitude

$$A^0 = -\bar{A}^0(\lambda_u^*, \lambda_t^*). \quad (13)$$

The $\rho \rightarrow \pi \pi$ vertex function is chosen to be of Breit-Wigner form,

$$\Gamma_{\rho \pi \pi}(m_{\pi \pi}) = \frac{g_{\rho \pi \pi}}{m_{\pi \pi}^2 - m_\rho^2 + i \Gamma_\rho m_\rho}, \quad (14)$$

where $m_\rho = 775.8$ MeV, the decay width is $\Gamma_\rho = 150.3$ MeV and the coupling constant is taken to be $g_{\rho \pi \pi}^2/4\pi = 3 m_\rho^2 \Gamma_\rho / 2p_\pi^3$.

C. Complete $B \rightarrow \pi \pi K$ decay amplitudes

We add the S -wave amplitude a_S of Ref. [7] for the $B \rightarrow (\pi \pi)_S K$ decays to obtain the complete decay amplitude as

$$\mathcal{M} = a_S + a_P |\mathbf{p}_\pi| |\mathbf{p}_K| \cos \theta, \quad (15)$$

where a_S is given by either Eq. (1) or Eq. (7) of Ref. [7] and a_P can be read either from Eq. (2) or Eq. (9) for B^- decays or for \bar{B}^0 decays, respectively. It follows from Ref. [7] and from Eqs. (8) and (13) that the S - and P -wave amplitudes a_S and a_P are related to their CP -conjugate amplitudes \bar{a}_S and \bar{a}_P by

$$\bar{a}_S = a_S(\lambda_u^*, \lambda_t^*), \quad \bar{a}_P = -a_P(\lambda_u^*, \lambda_t^*). \quad (16)$$

Thus, the conjugate of \mathcal{M} is written as

$$\bar{\mathcal{M}} = \bar{a}_S + \bar{a}_P |\mathbf{p}_\pi| |\mathbf{p}_K| \cos \theta. \quad (17)$$

In the amplitude a_S of the present work, the charming penguin contribution $C(m)$ of Ref. [7] is replaced by

$$C^S(m) = -(M_B^2 - m^2) f_K F_0^{B \rightarrow (\pi \pi)_S}(M_K^2)(\lambda_u S_u + \lambda_t S_t). \quad (18)$$

In Eq. (18), S_u and S_t are two complex parameters and $F_0^{B \rightarrow (\pi \pi)_S}(M_K^2) = 0.46$ [7] is the B -transition form factor to a pair of pions in an S -state. Furthermore, the constant χ , characteristic of the $f_0(980) \rightarrow \pi \pi$ decay, is fixed to 29.8 GeV^{-1} in agreement with the estimation made in Ref. [7]. Finally the effective coefficients $a_i(\mu = m_b/2)$ are now also taken from Ref. [21].

III. DEFINITIONS OF OBSERVABLES

The $B \rightarrow \pi \pi K$ amplitude \mathcal{M} in Eq. (15) depends on the effective mass $m_{\pi \pi}$ and $\cos \theta$ which is equivalent to the other effective mass variable $m_{\pi K}$ on the Dalitz plot. The double differential $B \rightarrow \pi \pi K$ decay distribution then reads

$$\frac{d^2 \Gamma}{d \cos \theta dm_{\pi \pi}} = \frac{m_{\pi \pi} |\mathbf{p}_\pi| |\mathbf{p}_K| |\mathcal{M}|^2}{8 (2\pi)^3 M_B^3}, \quad (19)$$

Integrating over $\cos \theta$ one obtains the differential $B \rightarrow \pi \pi K$ decay distribution

$$\frac{d\Gamma}{dm_{\pi \pi}} = \frac{m_{\pi \pi} |\mathbf{p}_\pi| |\mathbf{p}_K|}{4 (2\pi)^3 M_B^3} \left(|a_S|^2 + \frac{1}{3} |\mathbf{p}_\pi|^2 |\mathbf{p}_K|^2 |a_P|^2 \right) \quad (20)$$

and the differential branching ratio is given by

$$\frac{d\mathcal{B}}{dm_{\pi \pi}} = \frac{1}{\Gamma_B} \frac{d\Gamma}{dm_{\pi \pi}}, \quad (21)$$

where Γ_B is the appropriate total width for B^+ or B^0 .

The integration on the Dalitz plot over the kinematically allowed $m_{\pi \pi}$ range yields the helicity angle $B \rightarrow \pi \pi K$ distribution

$$\frac{d\Gamma}{d \cos \theta} = A + B \cos \theta + C \cos^2 \theta. \quad (22)$$

The functions A , B and C are defined as

$$A = \int_{m_{\min}}^{m_{\max}} \frac{m_{\pi \pi} |\mathbf{p}_\pi| |\mathbf{p}_K|}{8 (2\pi)^3 M_B^3} |a_S|^2 dm_{\pi \pi}, \quad (23)$$

$$B = 2 \int_{m_{\min}}^{m_{\max}} \frac{m_{\pi \pi} |\mathbf{p}_\pi|^2 |\mathbf{p}_K|^2}{8 (2\pi)^3 M_B^3} \text{Re}(a_S a_P^*) dm_{\pi \pi}, \quad (24)$$

$$C = \int_{m_{\min}}^{m_{\max}} \frac{m_{\pi \pi} |\mathbf{p}_\pi|^3 |\mathbf{p}_K|^3}{8 (2\pi)^3 M_B^3} |a_P|^2 dm_{\pi \pi}. \quad (25)$$

The CP violating asymmetry for charged B decays is defined as

$$\mathcal{A}_{CP} = \frac{\frac{d\Gamma(B^- \rightarrow \pi^+ \pi^- K^-)}{dm_{\pi \pi}} - \frac{d\Gamma(B^+ \rightarrow \pi^+ \pi^- K^+)}{dm_{\pi \pi}}}{\frac{d\Gamma(B^- \rightarrow \pi^+ \pi^- K^-)}{dm_{\pi \pi}} + \frac{d\Gamma(B^+ \rightarrow \pi^+ \pi^- K^+)}{dm_{\pi \pi}}}. \quad (26)$$

Furthermore, in neutral B meson decays into final CP eigenstates f the time-dependent asymmetries are given by

$$\begin{aligned}\mathcal{A}_{CP}(t) &= \frac{\Gamma(\bar{B}^0(t) \rightarrow f) - \Gamma(B^0(t) \rightarrow f)}{\Gamma(\bar{B}^0(t) \rightarrow f) + \Gamma(B^0(t) \rightarrow f)} \\ &= \mathcal{S} \sin(\Delta mt) + \mathcal{A} \cos(\Delta mt).\end{aligned}\quad (27)$$

The mass difference between the two neutral B eigenstates is denoted by Δm , \mathcal{S} is a measure for the mixing induced CP asymmetry, and \mathcal{A} is the direct CP violating asymmetry. The two parameters of the time dependent asymmetry, \mathcal{S} and \mathcal{A} , are

$$\begin{aligned}\mathcal{S} &= \frac{2 \operatorname{Im} \lambda_f}{1 + |\lambda_f|^2} = (1 - \mathcal{A}) \operatorname{Im} \lambda_f, \\ \mathcal{A} &= -\frac{1 - |\lambda_f|^2}{1 + |\lambda_f|^2},\end{aligned}\quad (28)$$

with

$$\lambda_f = e^{-2i\beta} \frac{\bar{\mathcal{M}}(\bar{B}^0 \rightarrow f)}{\mathcal{M}(B^0 \rightarrow f)} \quad (29)$$

and β being the CKM matrix angle. Inserting the corresponding $\mathcal{M}(\bar{B}^0 \rightarrow f)$ amplitude from Eq. (15) and $\bar{\mathcal{M}}(B^0 \rightarrow f)$ amplitude from Eq. (17) into Eqs. (28), one obtains after integration over $\cos \theta$ the integrated \mathcal{S} asymmetry

$$\begin{aligned}\mathcal{S}(m_{\pi\pi}) &= (1 - \mathcal{A}) \times \\ &\times 2 \operatorname{Im} \left\{ e^{-2i\beta} \left[\bar{a}_S a_S^* + \frac{1}{3} |\mathbf{p}_\pi|^2 |\mathbf{p}_K|^2 \bar{a}_P a_P^* \right] \right\} \quad (30)\end{aligned}$$

and the \mathcal{A} asymmetry integrated over $\cos \theta$ is

$$\mathcal{A}(m_{\pi\pi}) = \frac{|\bar{a}_S|^2 - |a_S|^2 + \frac{1}{3} |\mathbf{p}_\pi|^2 |\mathbf{p}_K|^2 (|\bar{a}_P|^2 - |a_P|^2)}{|\bar{a}_S|^2 + |a_S|^2 + \frac{1}{3} |\mathbf{p}_\pi|^2 |\mathbf{p}_K|^2 (|\bar{a}_P|^2 + |a_P|^2)}. \quad (31)$$

IV. FITTING PROCEDURE

In our fitting procedure we include the experimental data of Belle [1, 3, 23, 24] and BaBar [4, 5, 25, 26] Collaborations. They include altogether 18 values of branching fractions, direct CP violating asymmetries for the charged B decays and the time dependent CP asymmetry parameters \mathcal{S} and \mathcal{A} determined for the $B^0 \rightarrow \rho(770)K_S^0$ and $B^0 \rightarrow f_0(980)K_S^0$ decays. These data constitute the first part of the observable ensemble we fit. If one denotes by Z_i^{exp} and Z_i^{th} the experimental and theoretical value of the above mentioned observables and by ΔZ_i^{exp} their empirical errors, then the corresponding first part of the χ^2 function reads:

$$\chi_I^2 = W_I \sum_{i=1}^{18} \left[\frac{Z_i^{\text{exp}} - Z_i^{\text{th}}}{\Delta Z_i^{\text{exp}}} \right]^2. \quad (32)$$

TABLE I: Charming penguin parameters in the S -wave (S_u and S_t) and in the P -wave (P_u and P_t).

Parameter	Value
$ S_u $	0.15 ± 0.10
$\operatorname{Arg} S_u$	1.90 ± 0.71
$ S_t $	0.020 ± 0.002
$\operatorname{Arg} S_t$	-0.26 ± 0.21
$ P_u $	1.09 ± 0.21
$\operatorname{Arg} P_u$	-0.98 ± 0.12
$ P_t $	0.065 ± 0.002
$\operatorname{Arg} P_t$	-1.56 ± 0.08

Here, $W_I = 10$ is a weight factor chosen so as to make a good balance between this and the second component χ_{II}^2 of the total χ^2 function. The χ_{II}^2 function is defined similarly to Eq. (32) but for the observables Z_i being the $\pi\pi$ effective-mass and the helicity-angle distributions. We set $W_{II} = 1$. The experimental distributions have been background subtracted according to the figures of the Belle and BaBar papers cited above. For completeness, we give a list of figures showing the data we used in the evaluation of χ_{II}^2 : figures 5b, 6c, 6d and 7a till 7f from Ref. [23], figures 5c, 6c, 6d from Ref. [3], figure 3b from Ref. [5], and figure 3 from Ref. [4]. The experimental data are not absolutely normalized, therefore we have adopted an adequate method, described below, to compare the theoretical differential distributions of Eqs. (20) and (22) with the experimental $m_{\pi\pi}$ and $\cos \theta$ distributions.

For both differential distributions in $x = m_{\pi\pi}$ and $x = \cos \theta$, we define the theoretical number of events in a bin x_i by the integral

$$Y_{\text{th}}(x_i) = \mathcal{N} \Gamma_B^{-1} \int_{x_{i1}}^{x_{i2}} \frac{d\Gamma(x)}{dx} dx. \quad (33)$$

The differential model distribution $d\Gamma(x)/dx$ is just that given by either Eq. (20) or Eq. (22) and the integration range of the kinematic variables is the bin width $[x_{i1}, x_{i2}]$. Then the normalization coefficient \mathcal{N} of a given experimental distribution Y_{exp} is defined as a sum over all chosen bins:

$$\mathcal{N} = \Gamma_B \frac{\sum_{i=1}^n Y_{\text{exp}}(x_i)}{\int_{X_1}^{X_2} \frac{d\Gamma(x)}{dx} dx}. \quad (34)$$

The sum of experimental events $Y_{\text{exp}}(x_i)$ over x_i and the integration of $d\Gamma(x)/dx$ over x is done in the analyzed range $[X_1, X_2]$ of interest, which must be within the kinematically allowed range for the variables $m_{\pi\pi}$ and $\cos \theta$. Since we concentrate ourselves on the $\pi\pi$ effective mass range where the $\rho(770)^0$ and $f_0(980)$ resonances contribute the most, we take in our fits $X_1 = 0.60$ GeV and $X_2 = 1.06$ GeV.

The experimental branching fractions for charged and neutral $B \rightarrow \rho(770)^0 K$ and $B \rightarrow f_0(980) K$ decays are

TABLE II: Average branching fractions \mathcal{B} in units of 10^{-6} , asymmetries \mathcal{A}_{CP} , and the asymmetry parameters \mathcal{S} and \mathcal{A} of our model compared to the values of Belle and BaBar Collaborations. The experimental branching ratios and their errors have been multiplied by 0.71 for $B \rightarrow \rho K$ channels and by 0.69 for $B \rightarrow f_0 K$ channels (for explanation see Section IV).

Observable	Channel	$\pi^+ \pi^-$ mass range (GeV)	Our model	Belle	BaBar
				Ref.	Ref.
\mathcal{B}	$\rho^0 K^\pm$	(0.66, 0.90)	2.91 ± 0.10	2.76 ± 0.45	[1]
\mathcal{A}_{CP}	$\rho^0 K^\pm$	(0.66, 0.90)	0.32 ± 0.03	0.30 ± 0.14	[1]
\mathcal{B}	$f_0 K^\pm$	(0.90, 1.06)	6.93 ± 0.16	6.06 ± 1.08	[1]
\mathcal{A}_{CP}	$f_0 K^\pm$	(0.90, 1.06)	0.02 ± 0.02	-0.08 ± 0.08	[1]
\mathcal{B}	$\rho^0 K^0$	(0.66, 0.90)	3.49 ± 0.20	4.35 ± 1.05	[3]
\mathcal{B}	$f_0 K^0$	(0.90, 1.06)	3.86 ± 0.14	5.24 ± 1.28	[3]
\mathcal{S}	$\pi^+ \pi^- K_S^0$	(0.66, 0.90)	0.11 ± 0.11	—	0.17 ± 0.58
\mathcal{A}	$\pi^+ \pi^- K_S^0$	(0.66, 0.90)	0.01 ± 0.06	—	-0.64 ± 0.48
\mathcal{S}	$\pi^+ \pi^- K_S^0$	(0.89, 1.088)	-0.67 ± 0.05	-0.47 ± 0.37	[24]
\mathcal{S}	$\pi^+ \pi^- K_S^0$	(0.86, 1.10)	-0.63 ± 0.05		-0.95 ± 0.29
\mathcal{A}	$\pi^+ \pi^- K_S^0$	(0.89, 1.088)	-0.11 ± 0.07	-0.23 ± 0.26	[24]
\mathcal{A}	$\pi^+ \pi^- K_S^0$	(0.86, 1.10)	-0.11 ± 0.07		0.24 ± 0.34

obtained with the isobar model, in which the B -decay amplitude is a sum over the contributions of different two-body resonances. These are usually parameterized in terms of Breit-Wigner functions with the exception of the $f_0(980)$, for which the Flatté formula is used. After fitting the intensities of the resonances, a particular branching fraction for a given resonance is calculated as an integral over the fully available phase space on the Dalitz plot. In order to compare these experimental branching fractions with those for limited effective mass ranges, we have calculated appropriate reduction coefficients as the ratio of the integral over the limited phase space to that over the fully allowed one using the phenomenological amplitudes of the experimental analyses. They are equal to 0.71 in the case of the $\rho(770)^0$ and a $m_{\pi\pi}$ range $0.66 - 0.90$ GeV and to 0.69 for the $f_0(980)$ which dominates in the $0.90 - 1.06$ GeV range. In fitting our model to the data, these coefficients reduce the branching fractions and their errors by the same factor.

Experimental cuts on the effective pion-kaon mass influence the $\pi\pi$ effective-mass and the helicity angle distributions. A typical veto cut is experimentally used around the $K\pi$ effective mass, close to the D -meson mass. In our calculations, we have applied the cuts specified by the Belle and BaBar Collaborations in their analyses of the B decays into $\pi\pi K$.

Our model has four complex parameters: P_u and P_t in the P -wave amplitude and S_u and S_t in the S -wave amplitude. With these parameters we shall describe more than two hundred data values.

V. RESULTS

We have performed a global fit to the available data measured by BaBar and Belle. These consist of 204 data points describing the $\pi\pi$ mass and angular distributions

and of 18 observables enumerated in Section IV. The χ^2 values are the following: $\chi^2_I/W_I = 9.8$ and $\chi^2_{II} = 336.3$. The values of the eight real parameters are listed in Table I along with the parabolic errors from the MINUIT minimization procedure [27].

In Table II, the values of branching fractions, direct and time-dependent CP asymmetries are presented along with the corresponding experimental ones. The calculated observables for a given channel are integrated over the $m_{\pi\pi}$ range indicated in this table. Both the BaBar and Belle values are in agreement within their error bars and are well reproduced in our model. The theoretical errors stem from the parameter errors given in Table I.

We stress the importance of charming penguin terms. Without them it is not possible to obtain a good agreement of the theoretical branching ratios with experimental data. If all the penguin parameters are set equal to zero then the model branching ratio is underestimated by a factor of about 5 for the $B^0 \rightarrow f_0(980)K^0$ decay and by 3.5 for the $B^0 \rightarrow \rho(770)^0 K^0$ decay. For the charged B decays the theoretical branching ratios are too small by factors 7 and 2.4 for the $f_0(980)K$ and $\rho(770)^0 K$ channels, respectively.

A. The $\pi\pi$ mass and helicity-angle distributions in $B^\pm \rightarrow \pi^+ \pi^- K^\pm$ decays

In Fig. 2 the $\pi\pi$ effective-mass distributions of our model are compared to the Belle data [23]. In the fit to these distributions, the background corrected data have been used. One sees from Figs. 2a and 2b that our model describes rather well the $\pi^+ \pi^-$ spectra measured by the Belle Collaboration separately for the B^+ and B^- decays. Our theoretical curve depicts, as in previous work [7], a prominent maximum near 1 GeV, to which now adds a less pronounced peak at about 770–780 MeV.

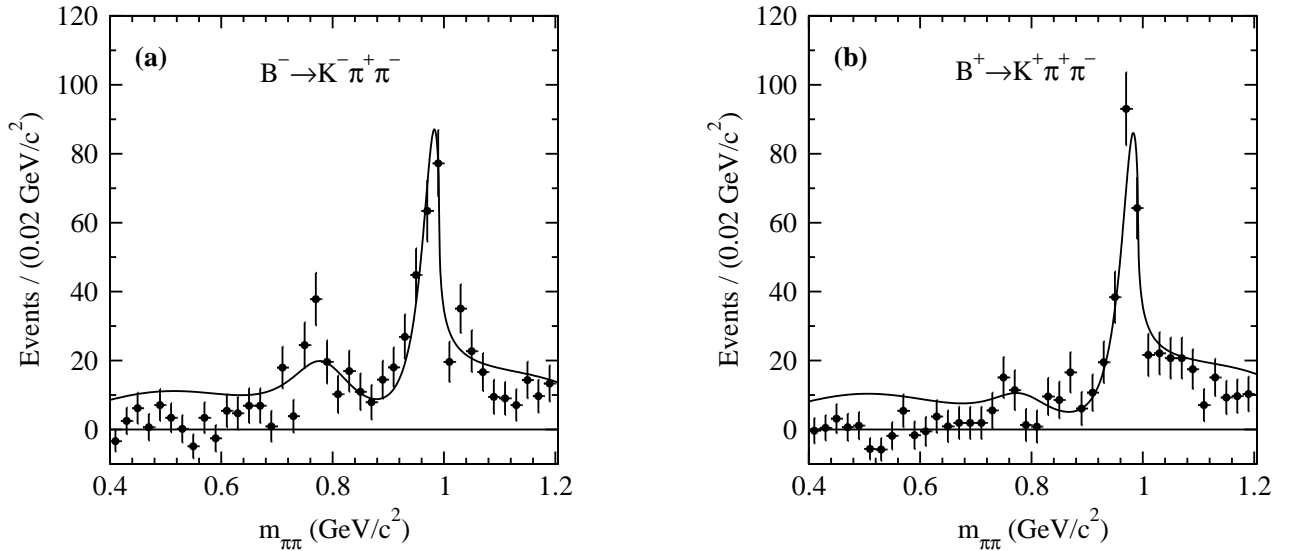


FIG. 2: The $\pi^+\pi^-$ effective-mass distributions (a) in $B^+ \rightarrow \pi^+\pi^-K^+$ and (b) in $B^- \rightarrow \pi^+\pi^-K^-$ decays. The data are taken from the Belle Collaboration [23]. The solid lines represent the results of our model.

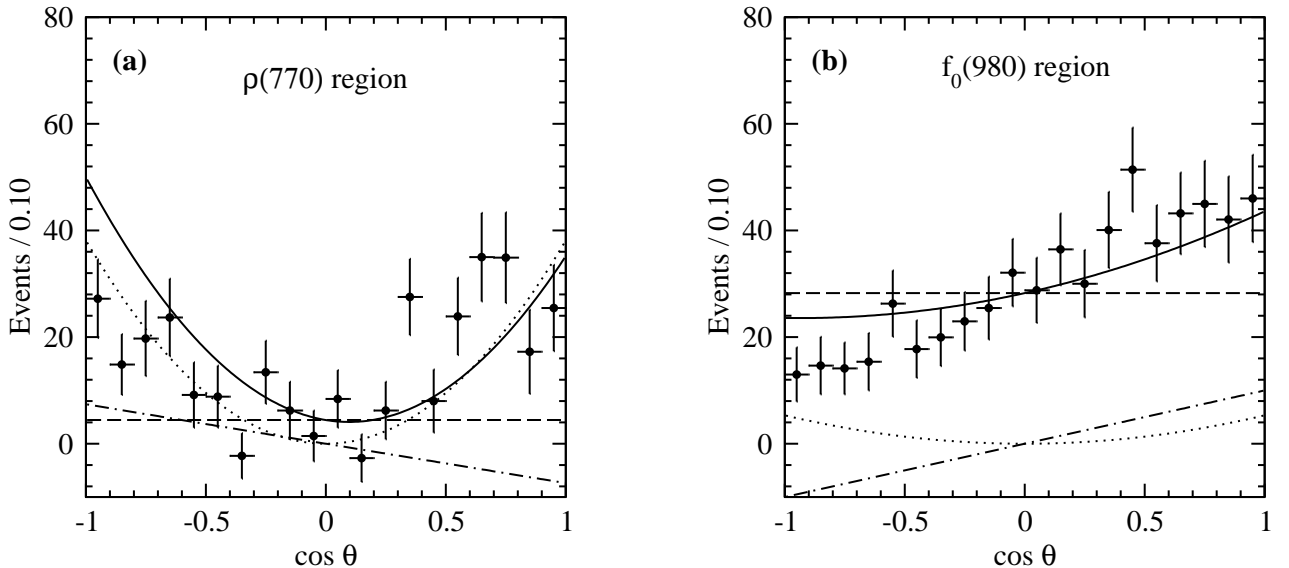


FIG. 3: Helicity-angle distributions in $B^\pm \rightarrow \pi^+\pi^-K^\pm$ (a) in the $\rho(770)$ mass region ($0.6 \text{ GeV} < m_{\pi\pi} < 0.9 \text{ GeV}$) and (b) in the $f_0(980)$ region ($0.9 \text{ GeV} < m_{\pi\pi} < 1.06 \text{ GeV}$). The data points are from Ref. [23] and the solid lines denote our model. The S -wave contribution is plotted with dashed lines, the P -wave with dotted lines and the interference term with dot-dashed lines.

Remarkably, one observes a clearly visible asymmetry in number of events between the $B^- \rightarrow K^-\pi^+\pi^-$ and $B^+ \rightarrow K^+\pi^+\pi^-$ decays for the $\rho(770)^0$ and $f_0(980)$ regions. At lower $m_{\pi\pi}$ masses about 500 MeV, our model also produces a broad maximum which we attribute to the σ or $f_0(600)$. By the same token, we note that in fits to their data, the Belle Collaboration has not included the σ resonance which is thus buried in the non-resonant background. Let us remark that this part of the $m_{\pi\pi}$ spectrum has not been fitted in our calculations. As explained in the previous section IV, we have intentionally

chosen the lower mass limit to be equal to 0.6 GeV.

In Fig. 3, we compare the results of our model for the $\cos\theta$ distribution in the vicinity of the $\rho(770)^0$ (Fig. 3a) and of the $f_0(980)$ (Fig. 3b) with the Belle data [23]. The experimental $\cos\theta$ distribution is fairly well reproduced given the fluctuation in events of the data points. The behavior of the angular distribution such as seen near the $f_0(980)$ mass is typical for a substantial interference pattern between the S - and P -wave. The former gives a constant contribution while the latter is a symmetric $\cos^2\theta$ distribution observed in the $\rho(770)^0$ mass range

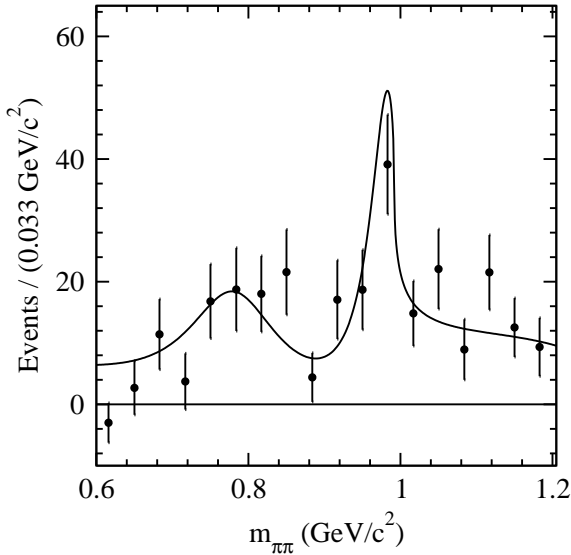


FIG. 4: The $\pi^+\pi^-$ effective-mass distributions in $B^0 \rightarrow \pi^+\pi^-K_S^0$ decays. Data points are taken from the BaBar Collaboration [5] while the continuous line results from our model.

(see Eq. (22)). The $S - P$ interference term, which is proportional to $\cos\theta$, is clearly seen in Fig. 3b. This demonstrates the presence of the P -wave contribution in the $f_0(980)$ region.

B. The $\pi\pi$ mass and helicity-angle distributions in $B^0 \rightarrow \pi^+\pi^-K^0$ decays

The $m_{\pi\pi}$ effective mass distribution for neutral B decays is plotted in Fig. 4 along with the results obtained by BaBar [5]. Within the error bars our model also describes this $m_{\pi\pi}$ distribution well, which bears the same features concerning the $\rho(770)^0$ and $f_0(980)$ as the charged B decay $m_{\pi\pi}$ spectrum. In Fig. 5a and 5b the $\cos\theta$ distributions in the proximity of the $\rho(770)^0$ and $f_0(980)$ are compared with the experimental data from Belle [3]. While the $\rho(770)^0$ range is dominated by the P -wave contribution, in the $f_0(980)$ range one observes once again the interference pattern. The sign of the interference term is, however, opposite to that apparent in Fig. 2b. It is well explained by our model in which the P -wave and S -wave amplitudes for both charged and neutral B decays are closely related (see Eqs. (3) and (10) where the signs of the charming penguin terms are reversed).

C. Interference effects

In this subsection we study the interplay between the S - and P -waves of the decay amplitudes. Fig. 6 shows the angular dependence of the two CP violating asymmetries \mathcal{S} and \mathcal{A} calculated at the effective masses $m_{\pi\pi} =$

775.8 MeV and $m_{\pi\pi} = 980$ MeV using Eqs. (28) and (29). These numbers are chosen to demonstrate the behavior of the asymmetries about the $\rho(770)^0$ and $f_0(980)$ resonances. As seen in Fig. 6a and 6b, the functions \mathcal{S} and \mathcal{A} are not constant. This is a clear demonstration of the interference between S - and P -waves. The sharp changes in behavior of the asymmetry \mathcal{S} at the $\rho(770)^0$ mass are shown in Fig. 6c, where the straight dashed and dotted lines are the \mathcal{S} values for separate S - and P -wave contributions, respectively. At $\cos\theta = 0$, the P -wave amplitude vanishes, therefore the strongest variations of the asymmetry are observed near $\theta = \pi/2$. A similar picture for the asymmetry \mathcal{A} is shown in Fig. 6d.

The asymmetries \mathcal{S} and \mathcal{A} at $m_{\pi\pi} = 980$ MeV behave smoothly near $\cos\theta = 0$ since there the S -wave dominates. A decrease of \mathcal{A} as well as an increase of \mathcal{S} as functions of $\cos\theta$ are due to the P -wave amplitude component, which is still non-negligible in the $f_0(980)$ mass range.

Recall that the helicity angle dependence of the asymmetries can be transformed into the functional dependence on the π^-K effective mass

$$m_{\pi^-K} = \sqrt{m_\pi^2 + m_K^2 + m_{\pi\pi}E_K(m_{\pi\pi}) + 2|\mathbf{p}_\pi||\mathbf{p}_K|\cos\theta}, \quad (35)$$

where m_π is the pion mass. Thus, the above interference effects can also be experimentally studied by examination of particular regions of the Dalitz plot.

In Fig. 7, the effective $\pi\pi$ mass dependence of the asymmetries integrated over $\cos\theta$ are plotted (see Eqs. (30) and (31)). The most pronounced effect is an intermediate change of sign of \mathcal{S} near the $\rho(770)^0$ resonance. We stress that if the S - or P -amplitudes were dominated by only one weak amplitude proportional to λ_t then the asymmetry \mathcal{S} shown in Fig. 7a would suddenly jump from $-\sin 2\beta \approx -0.7$ at the $\pi\pi$ threshold to $+\sin 2\beta \approx +0.7$ near the $\rho(770)^0$ mass and abruptly drop down to $-\sin 2\beta \approx -0.7$ at the $f_0(980)$ mass, as can be inferred from Eq. (30). A smooth behavior of \mathcal{S} is explained by the mass dependence of the S -wave scalar form factors and by the finite width of the $\rho(770)^0$. As seen in Fig. 7a, our model is in agreement with the data. Remarkably, there is a particularly large departure from the $+\sin 2\beta$ value near the $\rho(770)^0$ mass. This can be explained by a substantial value of the weak part of the amplitude in Eqs. (6) and (10) proportional to λ_u . In this context, bear in mind that the P -wave penguin parameter $|P_u|$ is much larger than the S -wave parameter $|S_u|$ (see Table I).

The functional dependence of the asymmetry \mathcal{A} on $m_{\pi\pi}$ is depicted in Fig. 7b. It is not as strong as for the \mathcal{S} asymmetry, but certainly \mathcal{A} is not equal to zero. In the $f_0(980)$ range, \mathcal{A} is close to -0.1 . Hence, it is comparable to the values of \mathcal{A} found by Belle and Babar in $B^0 \rightarrow K^+\pi^-$ decays [28, 29]. In the former case, however, the experimental errors are yet too large to claim the non-zero value of \mathcal{A} (see Table II).

We conclude this section by remarking that in pen-

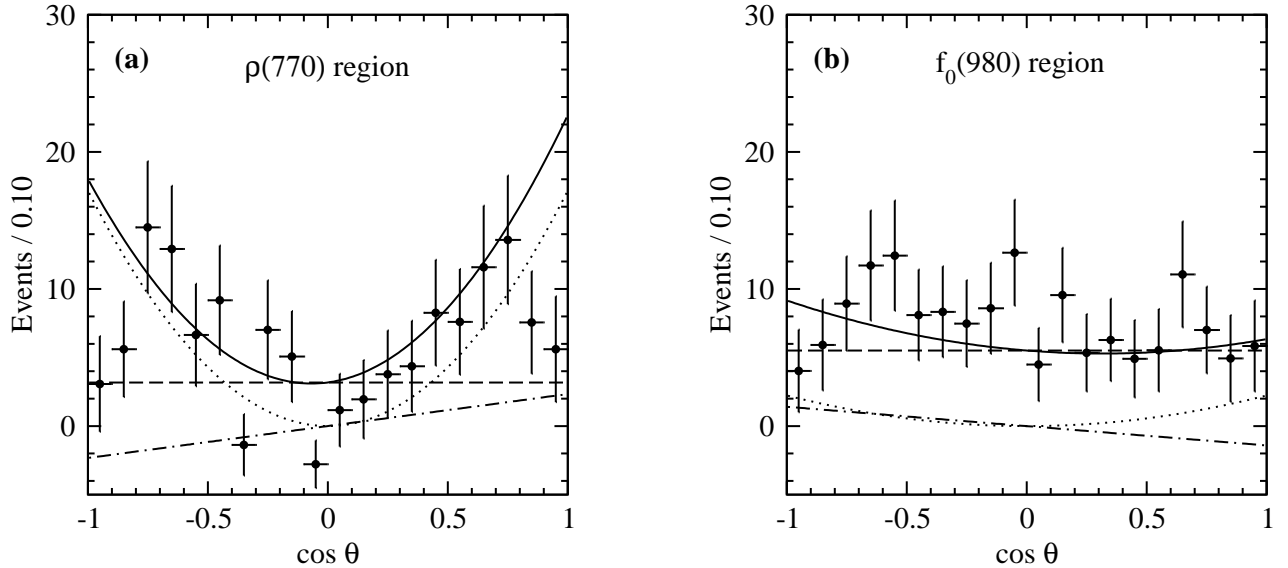


FIG. 5: As in Fig. 2 but for $B^0 \rightarrow \pi^+ \pi^- K_S^0$ decays and for data from Belle [3].

guin dominated decays, such as $B \rightarrow \rho K, \omega K, \dots$, tree diagrams are either CKM suppressed or CKM and color suppressed. Still, we observe that for $\rho(770)^0 K$ final states an accidental cancellation occurs in the λ_u terms of Eqs. (4) and (11) due to the combinations $a_4^c - r a_6^c$ and $a_4^u - r a_6^u$, where $r \simeq 1$, $a_6^{u,c} \approx a_4^{u,c}$. A similar cancellation takes place in the $B \rightarrow f_0(980) K$ channel [7]. Therefore, the ‘tree pollution’ is considerable and one may, at this point already, expect deviations from the value $\mathcal{S} \approx \sin 2\beta$ associated with the pure tree diagram for the $B^0 \rightarrow J/\psi K_S$ or with the penguin diagram for the $B^0 \rightarrow \phi K^0$ decays. The tree diagram contribution to the $\rho(770)^0 K$ state, however, is not sufficient to explain the important departure of \mathcal{S} from the above value. It is the aforementioned long-distance contribution $|P_u|$ to the λ_u term combined with interference effects that determine the functional behavior of the \mathcal{S} asymmetry parameter.

VI. CONCLUSIONS AND OUTLOOK

In our studies of $B \rightarrow \pi^+ \pi^- K$ decays, we have extended the work of Ref. [7] by adding the P -wave contribution to that of the S -wave in the two-pion final-state interactions. The total amplitude contains the resonant channels $B \rightarrow \rho(770)^0 K$ and $B \rightarrow f_0(980) K$. This work goes beyond the usual approach of calculating two-body branching ratios of the B decays, as we have taken into account parts of the final state interactions between particles in three-body decay channels. In this paper, we have analyzed the interactions between pairs of pions in the Dalitz plot section with the $\pi\pi$ effective mass range from threshold to about 1.2 GeV. In the S -wave the rescattering or the transition amplitudes between two pions or two kaons are described by the unitary coupled-channel model of Ref. [19].

There are two components in the weak transition amplitudes. The first term is derived within the factorization approximation with some QCD corrections without hard-scattering and annihilation terms. The second contribution, called charming penguins, is a long-distance amplitude originating from penguin-type diagrams with c -quark or u -quark loops. Four complex charming penguin parameters, common for B^+, B^-, B^0 and \bar{B}^0 decays, have been introduced and fitted to numerous experimental data, including the $\pi\pi$ effective mass and helicity angle distributions, branching fractions, direct asymmetry \mathcal{A}_{CP} and time dependent CP violating asymmetry parameters \mathcal{S} and \mathcal{A} . Our theoretical model reproduces well the experimental results. Without the charming penguin amplitudes, the model branching fractions of $B \rightarrow f_0(980) K$ and $B \rightarrow \rho(770)^0 K$ decays are several times smaller than the experimental values. In the $m_{\pi\pi}$ range below 1.2 GeV, the two main resonances $\rho(770)^0$ and $f_0(980)$ give rise to important interference effects, best visible in the helicity-angle distributions. Thus, in Figs. 3 and 5, we notice sizable interference terms of opposite signs comparing the $B^\pm \rightarrow \pi^+ \pi^- K^\pm$ decays with the $B^0 \rightarrow \pi^+ \pi^- K^0$ ones.

In our model, the direct CP asymmetry in $B^\pm \rightarrow \rho^0 K^\pm$ decays is in agreement with the large experimental value measured by the Belle and BaBar groups. The parameter \mathcal{S} of the time-dependent CP asymmetry for $B^0 \rightarrow \rho^0 K_S^0$ decays is significantly smaller than the value $\sin 2\beta$ expected in case of a full dominance of the weak decay amplitude proportional to λ_t . This is related to a large value of the u -penguin parameter P_u in the P -wave (see Table I). The numbers S_u , S_t , P_u and P_t should be treated as phenomenological parameters which we attribute to the long-distance penguin contributions. In our opinion, however, they can also contain contributions from other processes omitted by us like annihilation or

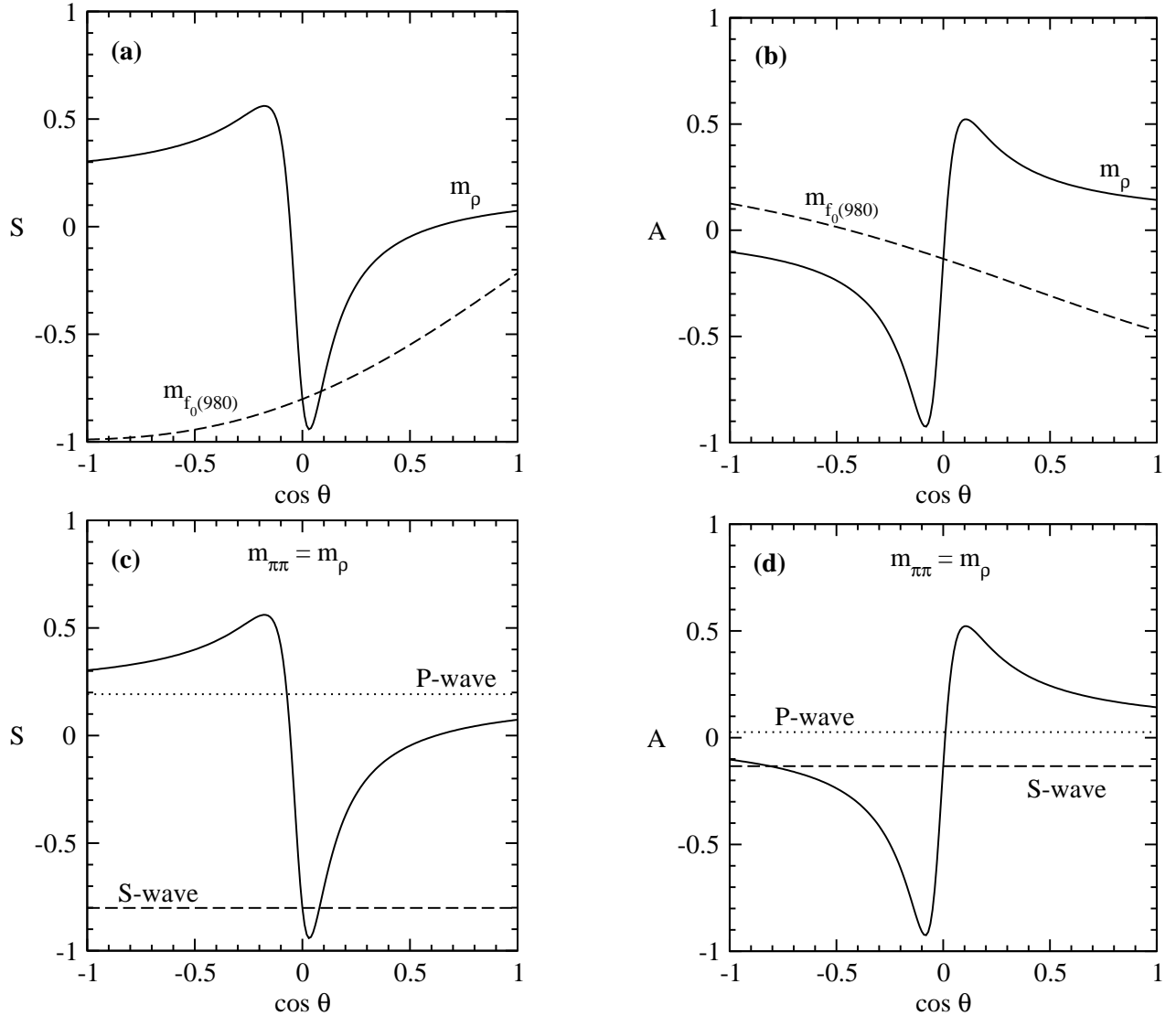


FIG. 6: Helicity-angle dependence of the CP violating asymmetries S and A calculated for $B^0 \rightarrow \pi^+\pi^-K_S^0$ decays at $m_{\pi\pi}$ equal to $m_\rho = 775.8$ MeV (solid lines in (a)–(d)) and to $m_{f_0(980)} = 980$ MeV (dashed lines in (a) and (b)). Separate S -wave (dashed lines) and P -wave results (dotted lines) are shown in (c) and (d) for $m_{\pi\pi} = m_\rho$.

hard-spectator interaction terms.

In this approach, all the resonances appear in a natural way as poles of the meson-meson amplitudes. No arbitrary phases nor any relative intensity parameters for the two discussed resonances $\rho(770)^0$ and $f_0(980)$ are needed. This is in contrast to the usual phenomenological analyses in terms of the isobar model applied to fit the Dalitz plot density distributions. Let us remark that the scalar resonance $f_0(600)$, as a pole of the S -wave amplitude, is also present in the $\pi\pi$ effective mass spectrum. However, it has not been included in the phenomenological models of the Belle and BaBar Collaborations [2, 4, 23].

So far, we have restricted our analysis to an effective $\pi\pi$ mass of about 1.2 GeV. In further studies, one can extend not only this mass range to include further scalar and vector resonances but also treat the other variable

$m_{\pi K}$ on the Dalitz plot and the accompanying vector resonances K^* . Given our findings for the $f_0(980)$ and $\rho(770)^0$ resonances, we expect many more interference effects at larger effective $\pi\pi$ masses and also for the πK effective mass range.

Acknowledgments

One of us (L. L.) is very grateful to Maria Różańska for many useful conversations and remarks on B -meson decays. B.E. is thankful to Thomas Latham for providing access to the BaBar raw data on effective mass distributions including background corrections. B.E. and B.L. acknowledge pleasant and helpful discussions with José Ocariz and also thank Olivier Leitner for quite useful

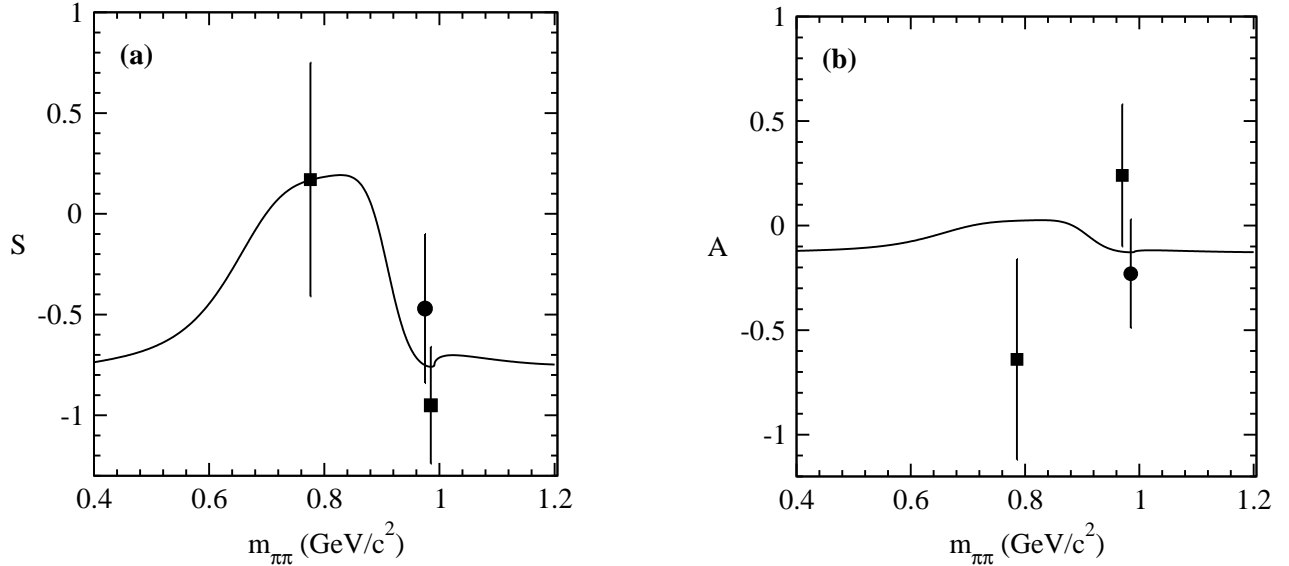


FIG. 7: Effective-mass dependence of the CP violating asymmetries, integrated over $\cos\theta$, S in (a) and A in (b) obtained with our model (solid lines). The Belle Collaboration results [24] for the $f_0(980)$ resonance are plotted as circles and the BaBar data for the $f_0(980)$ [25] and $\rho(770)^0$ [26] as squares.

comments.

This work has been performed within the framework of the IN2P3-Polish Laboratories Convention (Project No. CSI-12). A visit of B. E. in Kraków has been partly fi-

nanced within an agreement between the CNRS (France) and the Polish Academy of Sciences (Project No. 19481). B. E. is supported by a Marie Curie International Reintegration Grant under the Contract No. 516228.

[1] A. Garmash *et al.*, Belle Collaboration, hep-ex/0512066, *Evidence for large direct CP violation in $B^\pm \rightarrow \rho(770)^0 K^\pm$ from analysis of the three-body charmless $B^\pm \rightarrow K^\pm \pi^\pm \pi^\mp$ decay.*

[2] A. Garmash, *et al.*, Belle Collaboration, Phys. Rev. D **71** (2005) 092003, *Dalitz analysis of the three-body charmless decays $B^\pm \rightarrow K^\pm \pi^+ \pi^-$ and $B^\pm \rightarrow K^\pm K^+ K^-$.*

[3] K. Abe, *et al.*, Belle Collaboration, hep-ex/0509047, *Dalitz analysis of the three-body charmless decay $B^0 \rightarrow K_S^0 \pi^+ \pi^-$.*

[4] B. Aubert, *et al.*, BaBar Collaboration, Phys. Rev. D **72** (2005) 072003, *Dalitz-plot analysis of the decays $B^\pm \rightarrow K^\pm \pi^\mp \pi^\pm$.*

[5] B. Aubert, *et al.*, BaBar Collaboration, Phys. Rev. D **73** (2006) 031101(R), *Measurements of neutral B decay branching fractions to $K_S^0 \pi^+ \pi^-$ final states and the charge asymmetry of $B^0 \rightarrow K^{*+} \pi^-$.*

[6] B. Aubert, *et al.*, BaBar Collaboration, hep-ex/0408079, *Evidence for $B^0 \rightarrow \rho^0 K_S^0$.*

[7] A. Furman, R. Kamiński, L. Leśniak and B. Loiseau, Phys. Lett. B **622** (2005) 207, *Long-distance effects and final state interactions in $B \rightarrow \pi \pi K$ and $B \rightarrow K \bar{K} K$ decays.*

[8] M. Ciuchini, E. Franco, G. Martinelli and L. Silvestrini, Nucl. Phys. B **501** (1997) 271, *Charming penguins in B decays.*

[9] H. Y. Cheng, C. K. Chua and A. Soni, Phys. Rev. D **71** (2005) 014030, *Final state interactions in hadronic B de-*

cays, Phys. Rev. D **72** (2005) 014006, *Effects of final-state interactions on mixing-induced CP violation in penguin-dominated B decays.*

[10] H. Y. Cheng, C. K. Chua and K. C. Yang, Phys. Rev. D **73** (2006) 014017, *Charmless hadronic B decays involving scalar mesons: Implications on the nature of light scalar mesons.*

[11] C. M. Arnesen, Z. Ligeti, I. Z. Rothstein and I. W. Stewart, hep-ph/0607001, *Power corrections in charmless nonleptonic B -decays: annihilation is factorizable and real.*

[12] Ch. W. Bauer, D. Pirjol, I. Z. Rothstein and I. W. Stewart, Phys. Rev. D **70** (2004) 054015, *$B \rightarrow M_1 M_2$: Factorization, charming penguins, strong phases, and polarization.*

[13] M. Beneke, G. Buchalla, M. Neubert and C.T. Sachrajda, Phys. Rev. D **72** (2005) 098501, *Comment on " $B \rightarrow M_1 M_2$: Factorization, charming penguins, strong phases, and polarization".*

[14] O. Leitner, X. H. Guo and A. W. Thomas, J. Phys. G **31** (2005) 199, *Direct CP violation, branching ratios and form factors $B \rightarrow \pi$, $B \rightarrow K$ in B decays.*

[15] M. Beneke and M. Neubert, Nucl. Phys. B **675** (2003) 333, *QCD factorization for $B \rightarrow PP$ and $B \rightarrow PV$ decays.*

[16] G. Buchalla, G. Hiller, Y. Nir and G. Raz, JHEP **0509** (2005) 074, *The pattern of CP asymmetries in $b \rightarrow s$ transitions.*

- [17] M. Beneke, Phys. Lett. B **620** (2005) 143, *Corrections to $\sin 2\beta$ from CP asymmetries in $B^0 \rightarrow (\pi^0, \rho^0, \eta, \eta', \omega, \phi)K_S$ decays.*
- [18] N. de Groot, W. N. Cottingham and I. B. Whittingham, Phys. Rev. D **68** (2003) 113005, *Factorization fits and the unitarity triangle in charmless two-body B decays.*
- [19] R. Kamiński, L. Leśniak and B. Loiseau, Phys. Lett. B **413** (1997) 130, *Three channel model of meson meson scattering and scalar meson spectroscopy.*
- [20] U. G. Meissner and J. A. Oller, Nucl. Phys. A **679** (2001) 671, *$J/\psi \rightarrow \phi\pi\pi(K\bar{K})$ decays, chiral dynamics and OZI violation.*
- [21] M. Beneke, G. Buchalla, M. Neubert and C. T. Sachrajda, Nucl. Phys. B **606** (2001) 245, *QCD factorization in $B \rightarrow \pi K, \pi\pi$ decays and extraction of Wolfenstein parameters.*
- [22] J. Charles et al., CKMfitter Group, Eur. Phys. J. C **41** (2005) 1, *CP violation and the CKM matrix: assessing the impact of the asymmetric B factories.*
- [23] K. Abe et al., Belle Collaboration, hep-ex/0509001, *Search for direct CP violation in three body charmless $B^{\pm} \rightarrow K^{\pm}\pi^{\pm}\pi^{\mp}$ decays.*
- [24] K. Abe et al., Belle Collaboration, hep-ex/0507037, *Time dependent CP asymmetries $b \rightarrow \bar{q}q$ transitions and $\sin 2\Phi_1$ in $B^0 \rightarrow J/\Psi K^0$ decays with 386 million $B\bar{B}$ pairs.*
- [25] B. Aubert et al., BaBar Collaboration, hep-ex/0408095, *A measurement of CP violating asymmetries in $B^0 \rightarrow f_0(980)K_S^0$ decays.*
- [26] BaBar Collaboration, in preparation, cited by Heavy Flavor Averaging Group, April 2006.
- [27] F. James and M. Roos, Comput. Phys. Commun. **10** (1975) 343, *Minuit – a system for function minimization and analysis of the parameter errors and correlations.*
- [28] B. Aubert et al., BaBar Collaboration, Phys. Rev. Lett. **93** (2004) 131801, *Direct CP violating asymmetry in $B^0 \rightarrow K^+\pi^-$ decays.*
- [29] K. Abe et al., Belle Collaboration, hep-ex/0507045, *Improved measurements of direct CP violation in $B \rightarrow K^+\pi^-, K^+\pi^0$ and $\pi^+\pi^0$ decays.*